

Characterization of hexagonal defects in gallium nitride on sapphire

J. Kim^{a,*} and K.H. Baik^a

^aDepartment of Chemical & Biological Engineering, Korea University, Anam-dong, Sungbuk-gu, Seoul 136-701, Korea

^bSamsung Advanced Institute of Technology, Nongseo-dong, Giheung-gu, Younggin-si, Gyunggi 449-712, Korea

Hexagonal pits on the surface of GaN grown by an HVPE technique were characterized by SEM, CL-imaging, and micro-Raman scattering techniques. From the CL-imaging, there was seen to be a bright ring around the hexagonal pits, thereby implying disuniformities in the crystal surrounding the hexagonal pits. Then, micro-Raman techniques were employed for detailed analysis both inside and outside the hexagonal pits. E_2^2 phonons were monitored in order to characterize the strain. The film became more tensile by 0.13 GPa when the laser beam was scanned from the outside of the bright ring shown in the CL-imaging to the center of the hexagonal pit.

Key words: Gallium Nitride, Defects, SEM.

Introduction

GaN has shown outstanding potential for high power and high temperature applications in advanced communications and sensor technologies [1-3]. Also, the applications of this material system in optoelectronic devices including light emitting diodes (LED), and laser-diodes (LD) are currently the focus of a great deal of interest [4, 5]. Furthermore, recent advances in GaN-based spintronic devices have attracted a large amount of attention because high quality GaN film doped with Gd, Cr, and Mn can be grown, or these rare-earth elements can be implanted into the GaN layer [6-10]. GaN-based devices demonstrated that they are able to outperform the conventional Si-based and GaAs-based devices under harsh environments, but the lack of large, lattice-matched homoepitaxial substrates constitute the principal obstacle to the commercialization of these GaN-based devices. A variety of growth techniques including Molecular Beam Epitaxy (MBE), Metal Organic Chemical Vapor Deposition (MOCVD), and Hybrid Vapor Phase Epitaxy (HVPE) have been applied to the production of high-quality GaN epitaxial layers [11-13]. In our research, we have attempted to characterize a GaN layer grown by an HVPE technique, which can grow thicker and larger areas of GaN more rapidly than other techniques [14]. With regard to the quasi-bulk growth of GaN, thick GaN layers have been demonstrated on sapphire substrate with good electrical properties [14, 15]. The HVPE technique can also be an alternative to high temperature, high pressure bulk crystal growth, but the

GaN grown by an HVPE technique has various defects such as cracks, pinholes and hexagonal pits [16]. Hexagonal pits commonly form on the surface of HVPE GaN. These defects limit the performance and threaten the reliability of GaN-based devices. Because the structural, electrical, and optical properties of GaN grown by an HVPE technique rely on the growth conditions, the characterization of GaN using various techniques is important to optimize the quality of GaN and growth conditions.

Raman scattering is a non-destructive and contact-free technique which is used for the characterization of various semiconductors. The spatial resolution of the micro-Raman scattering technique is typically ≤ 2 micrometers. Considering that phonon frequencies are sensitive to the sample doping concentrations, as well as the strain and temperature conditions of semiconductors, Raman spectroscopy permits the monitoring and measurement of these essential semiconductor properties [17, 18].

In this paper, we describe the result of SEM, CL-imaging, and micro-Raman spectroscopy on hexagonal pits in the surface of a GaN layer grown on a sapphire substrate.

Experimentals

GaN was grown on a sapphire substrate by an HVPE technique. Micro-Raman scattering measurements were performed on the GaN in a backscattering geometry using the 488 nm line of an Ar-ion laser. The charge-coupled devices (CCDs) of the spectrometer were cooled with liquid nitrogen. The laser spot size was ≤ 3 μ m and the laser power at the sample was ~ 0.5 mW. The bandgap of GaN was larger than the incident photon energy, thereby minimizing possible laser-induced heat-

*Corresponding author:
Tel : +82-2-3290-3291
Fax: +82-2-926-6102
E-mail: hyunhyun7@korea.ac.kr

ing. GaN has a hexagonal Wurtzite structure. Due to its higher relative intensity at this scattering geometry, as well as its sensitivity to stress, we selected E_2^2 as a probe to monitor the biaxial strain in the GaN layer.

Initially, the GaN sample was characterized by SEM to find the hexagonal pits. After locating the hexagonal pits, a CL detector was employed in order to obtain an image at the same position. With the detailed image of the hexagonal pit, micro-Raman techniques were employed in order to characterize the changes in the strain both inside and outside the hexagonal pits.

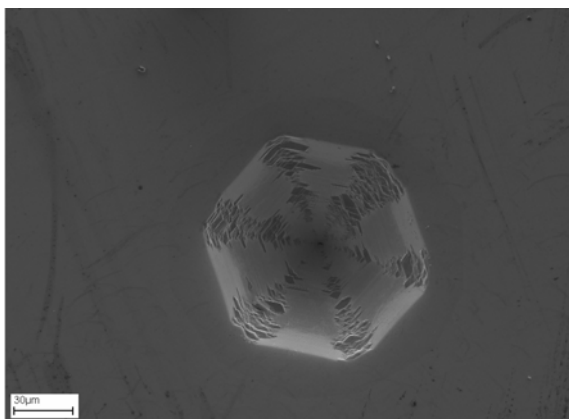
Results and Discussions

Figures 1(A) and 2(A) show that the defect looks like an inverted pyramid of hexagonal shape. CL-images (Fig. 1(B) and 2(B)) also indicate a ring-shaped grain-boundary around the hexagonal defect, which began to grow below the surface. Therefore, the properties of the crystal layer within the grain boundary (bright area in Fig. 1(B) and 2(B)) differ from those of the layer outside the grain boundary (dark area in Fig. 1(B) and 2(B)). Some reports have speculated about the origin of

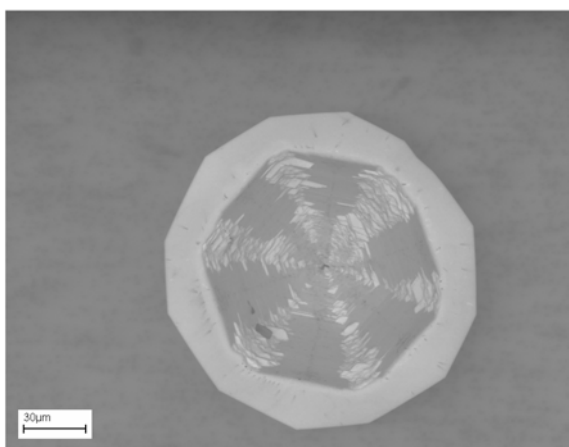
these hexagonal-shaped pits, and have principally attributed this phenomenon to dislocations [19]. In this study, we have employed micro-Raman scattering techniques, which allow us to obtain information regarding crystal structures and biaxial strain. We moved the position of the laser beam ($\sim 2 \mu\text{m}$ beam size) from outside the grain boundary to the center of the hexagonal pits. Figure 3 shows the micro-Raman Scattering data acquired from the defect-free area. We chose the E_2^2 phonon to monitor the biaxial strain because it is the most intense and is very sensitive to strain in the thin film in this backscattering geometry. When the laser beam was scanned from the outside of the ring to the center of the hexagonal pit, we determined that the film became more tensile (Fig. 4). Lorentzian fitting was employed to locate the peak position of the E_2^2 phonon, which was decreased by 0.8 cm^{-1} from the outside to the inside. There is a relationship between Raman shift and biaxial stress [20]:

$$s = \Delta\omega/6.2 \text{ cm}^{-1}\text{GPa}^{-1}$$

where s is the biaxial stress in GPa and $\Delta\omega$ is the

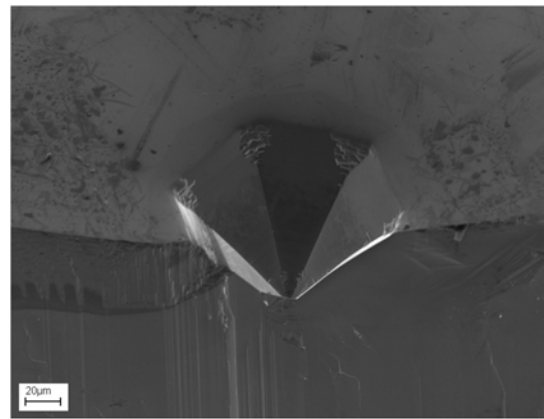


(A)

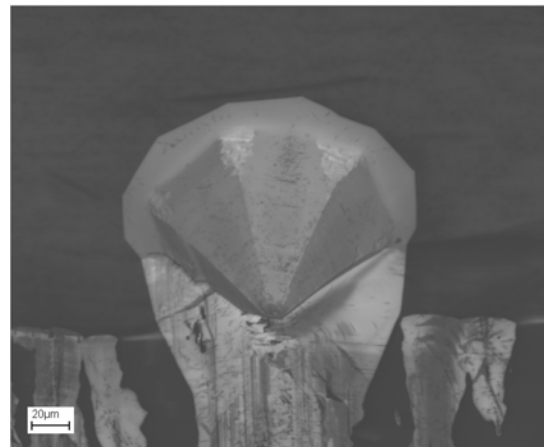


(B)

Fig. 1. (A) SEM micrograph of an hexagonal pit on the surface of GaN at 7 kV EHT, 17 mm working distance (Top View). (B) CL image of an hexagonal pit on the surface of GaN at 7 kV EHT, 17 mm working distance (Same position as Figure 1(A))



(A)



(B)

Fig. 2. (A) Cross-sectional SEM micrograph of an hexagonal pit at 10 kV EHT, 16 mm working distance. (B) Cross-sectional CL image of an hexagonal pit at 10 kV EHT, 16 mm working distance (Same position as Figure 2(A))

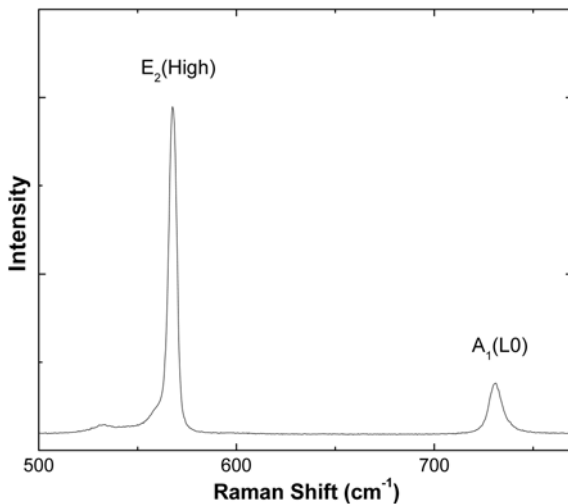


Fig. 3. Micro-Raman Scattering data taken far from a hexagonal pit (good area).

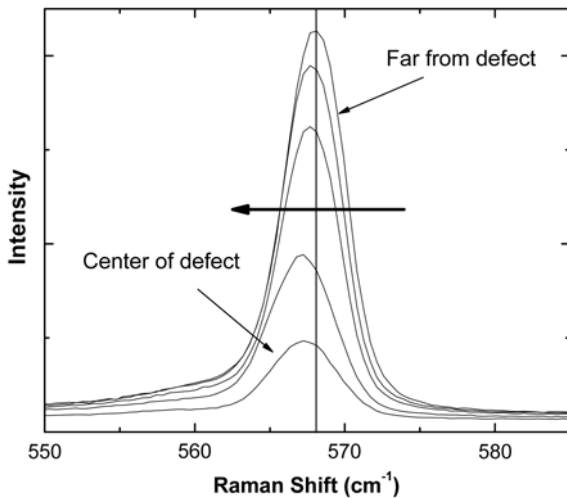


Fig. 4. E_2^2 phonon frequency change from a good area to the center of an hexagonal pit.

Raman Shift in cm^{-1} . Therefore 0.13 GPa of biaxial stress exists between the center of the hexagonal pit and the outer area.

The origin of hexagonal pits has been attributed to dislocations [19] although there is no convincing evidence yet. Paskova et al. mentioned that the electron concentration inside the defect is much higher than that outside the defect [21]. This can explain the difference in CL image contrast.

Figure 2(B) shows that the hexagonal defects terminate higher than other defects, which would have less effect on the performance of lateral devices (for example, lateral high power/high breakdown voltage rectifiers, Metal-Semiconductor Field Effect Transistors (MESFET), or AlGaIn/GaN High Electron Mobility Transistors (HEMT)) compared with the hexagonal pits. Therefore, optimization to minimize these hexagonal defects on GaN surfaces is very important for the maximization of the performance and yield of GaN-based devices.

Conclusions

In this study, SEM and CL-image were employed in order to characterize the hexagonal pits on GaN surface. Cross-sectional SEM and CL-images showed that the hexagonal pits were V-shaped and that they began to grow below the surface. When micro-Raman spectroscopy was used to characterize the strain in the GaN layer around an hexagonal pit, it was determined that the GaN layer became more tensile from the outer reference area to the center of the hexagonal pit by 0.13 GPa.

Acknowledgements

The Research at Korea University was supported by Brain Korea 21 Program in 2006.

References

1. L.F. Eastman, J.R. Shealy, V. Tilak, J. Smart, B. Green, and T. Prunty, In Proc 4th Int Conf Nitride Semiconduct Conf Dig Denver, CO, July, 16 (2001).
2. Y.-F. Wu, A. Saxler, M. Moore, R.P. Smith, S. Sheppard, and P.M. Chavarkar, IEEE Electron Dev. Lett 25 (2004) 117-119.
3. A.L. Spetz, A. Baranzahi, P. Tobias, and I. Lundstrom, Phys Status Solidi A 162 (1997) 493-511.
4. F.A. Ponce and D.P. Bour, Nature 386 (1997) 351-359.
5. S. Nakamura, T. Mukai, and M. Senoh, J. Appl. Phys. 76 (1994) 8189-8191.
6. G.T. Thaler, R.M. Frazier, C.R. Aberanty, and S.J. Pearton, Appl. Phys. Lett. 86 (2005) 131901-131902.
7. R.M. Frazier, J. Stapleton, G.T. Thaler, C.R. Abernathy, S.J. Pearton, R. Rairigh, J. Kelly, A.F. Hebard, M.L. Nakarmi, K.B. Nam, J.Y. Lin, H.X. Jiang, J.M. Zavada, and R.G. Wilson, J. Appl. Phys. 94 (2003) 1592-1596.
8. S.J. Pearton, C.R. Abernathy, M.E. Overberg, G.T. Thaler, D.P. Norton, N. Theodoropoulou, A.F. Hebard, Y.D. Park, F. Ren, J. Kim, and L.A. Boatner, J. Appl. Phys. 93 (2003) 1-13.
9. S.J. Pearton, M.E. Overberg, G. Thaler, C.R. Abernathy, N. Theodoropoulou, A.F. Hebard, S.N.G. Chu, R.G. Wilson, J. M. Zavada, A.Y. Polykov, A.V. Osinsky, P.E. Norris, P.P. Chow, A.M. Wowchack, J.M. Van Hove, and Y.D. Park, J. Vacuum Science & Technology A 20 (2002) 721-724.
10. G.T. Thaler, M.E. Overberg, B. Gila, R. Frazier, C.R. Abernathy, S.J. Pearton, J.S. Lee, S.Y. Lee, Y.D. Park, Z.G. Khim, J. Kim, and F. Ren, Appl. Phys. Lett. 80 (2002) 3964-3966.
11. T.D. Moustakas, T. Lei, and R.J. Molnar, Physica B 185 (1993) 36-49.
12. S. Nakamura, Japanese Journal of Applied Physics 30 (1991) L1705-L1707.
13. C.E.C. Dam, A.P. Grzegorzczak, P.R. Hageman, and P.K. Larsen, J. of Crystal Growth 290 (2006) 473-478.
14. R.J. Molnar, W. Gotz, L.T. Romano, and N.M. Johnson, J. Crystal Growth 178 (1997) 147-156.
15. M.A. Mastro, D. Tsvetkov, V. Soukhoveev, A. Usikov, V. Dmitriev, B. Luo, F. Ren, K.H. Baik, and S.J. Pearton, Solid-State Electronics 48 (2004) 179-182.
16. J. Jasinski and Z. Liliental-Weber, Journal of Electronic

- Materials 31 (2002) 429-436.
17. C. Wetzel, W. Walukiewicz, E.E. Haller, J. Ager III, I. Grzegory, S. Porowski, and T. Suski, Physical Review B 53 (1996) 1322-1326.
 18. T. Kozawa, T. Kachi, H. Kano, H. Nagase, N. Koide, and K. Manabe, Journal of Applied Physics 77 (1995) 4389-4392.
 19. T. Kozawa, T. Kaxhi, T. Ohwaki, Y. Taga, N. Koide, and M. Koide, Journal of Electrochemical Society 143 (1996) L17-L19.
 20. W. Rieger, T. Metzger, H. Angerer, R. Dimitrov, O. Ambacher, and M. Stutzmann, Appl. Phys. Lett. 68[7] (1996) 970-972.
 21. T. Paskova, E.M. Goldys, and B. Monemar, Journal of Crystal Growth 203 (1999) 1-11.